J. Fluid Mech. (1983), *vol.* 134, *pp.* 49–66
Printed in Great Britain

On the organized motion of a turbulent plane jet

By R. A. ANTONIA, L. W. B. BROWNE, S. RAJAGOPALAN AND A. J. CHAMBERS

Department of Mechanical Engineering, University of Newcastle, N.S.W. 2308, Australia

(Received 9 August 1982 and in revised form 19 April 1983)

Measurements of space–time correlations of longitudinal and normal velocity fluctuations and of temperature fluctuations support the existence of counter-rotating spanwise structures appearing alternately on opposite sides of the jet centreline in the self-preserving region of the flow. The frequency of these structures closely satisfies self-preservation. The asymmetric arrangement of the structures is first observed downstream of the position where the jet mixing layers nominally merge but upstream of the onset of self-preservation. Closer to the jet exit, the space–time correlations indicate the existence of spanwise structures that are symmetrical about the centreline.

1. Introduction

Oler & Goldschmidt (1981) have recently noted that the strongest indication of an ordered structure in the self-preserving region of a plane jet is the well-documented, although controversial, apparent flapping of a jet into still air.

Supporters of flapping, Goldschmidt & Bradshaw (1973) correlated instantaneous longitudinal velocity fluctuations on opposite sides of the centreline. They interpreted the quasiperiodic (in time) correlation and the negative value of this correlation at zero time delay to indicate significant flapping of the jet. Uberoi & Singh's (1975) instantaneous temperature profiles, obtained by shooting a cold wire across a section of a plane jet, appeared to indicate a flag-like flapping motion in the self-preserving region of the jet. Everitt & Robins (1978) presented correlations of the instantaneous streamwise velocity with separations in the x- and y-directions (figure 1). For a jet into still air, the lateral (y-separation) correlations became distinctly negative whenever the fixed and moving probes were on opposite sides of the jet centreline. This behaviour, also reported by Gutmark & Wygnanski (1976), Cervantes & Goldschmidt (1981) and Mumford (1982), is in contrast with the lateral correlations in the wake (Grant 1958), which did not become negative. Everitt & Robins (1978) interpreted these measurements as indicating a substantial degree of correlation between the large-scale motion on either side of the centreline and described the large-scale motion as local flapping. When the jet is exhausted into a moving external stream, the lateral correlations of Everitt & Robins (1978) and Bradbury (1965) did not exhibit the negative lobes revealed in the correlations for a jet into still air. Local flapping could thus be eliminated by the presence of even a weak external stream.

On the basis of the negligible correlation between intermittency functions obtained at approximately the mean interface locations on opposite sides of the centreline, Wygnanski & Gutmark (1971) concluded that the boundaries of a plane jet moved independently of each other. A similar conclusion was obtained by Moum, Kawall

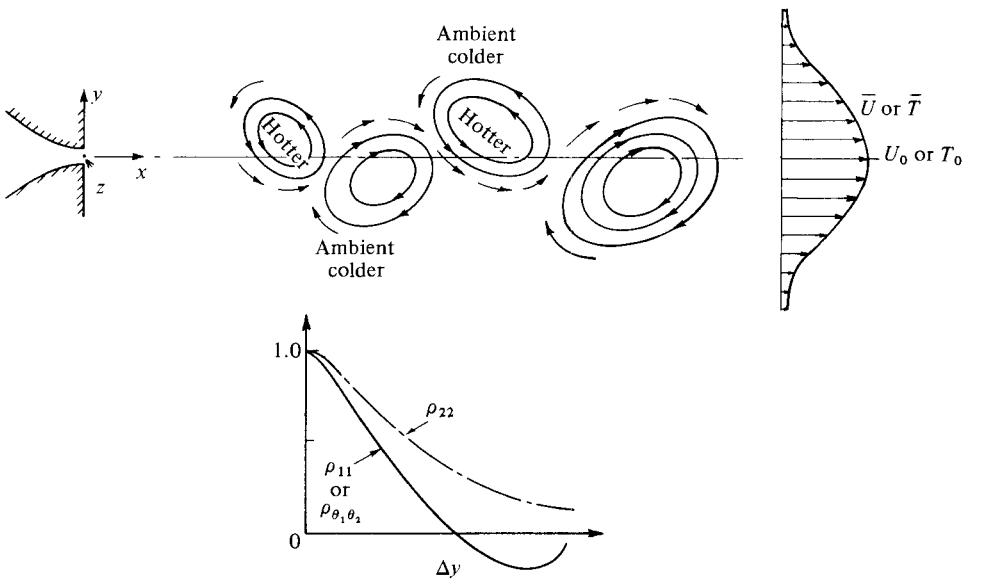

FIGURE 1. Schematic arrangement of spanwise structures in plane jet and associated lateral correlations when one probe is fixed on one side of the centreline and the other probe is located Δy away in the y-direction. Origin of axes is at the jet centreplane.

& Keffer (1979). The apparent conflict between this conclusion and apparent flapping led List (1982) to suggest that the evidence for either flapping or puffing, as against the independent motion of the jet boundaries, is equivocal.

Cervantes & Goldschmidt's (1981) suggestion that the apparent flapping was a characteristic of the organised motion in the jet was supported by several types of correlations of the velocity u obtained with single hot wires placed on opposite sides of the centreline. The frequency of flapping was found to scale with the centreline mean velocity and jet half-width. Oler (1980) and Oler & Goldschmidt (1981, 1982) evaluated the possibility that this motion can be represented by an essentially two-dimensional von Kármán vortex-street pattern, as sketched in figure 1. The size of the structures in this pattern was found to increase with x in conformity with self-preservation.

Lateral correlations (obtained with one probe fixed on one side of the jet centreline and another traversed in the y-direction at the same x-location) that may be compatible with the schematic flow pattern of figure 1 are shown in that figure. The correlation coefficient ρ_{11} (defined in §2) between u-fluctuations conforms with that obtained by other investigators. The expected coefficient ρ_{22} between v-fluctuations would remain positive, as the inward motion of fluid towards the centreline should, on average, be positively correlated with an outward motion on the other side of the centreline. When the jet is slightly heated, the correlation $\rho_{\theta_1\theta_2}$ between temperature fluctuations should follow, at least qualitatively, the same behaviour as ρ_{11}. When the distance between the probes is sufficiently large, $\rho_{\theta_1\theta_2}$ should be negative, since the inward and outward motions mentioned previously would be associated with colder and hotter fluid respectively. Correlations, with respect to time or x, obtained with two probes on opposite sides of the centreline should reflect the streamwise periodicity of the patterns in figure 1.

One aim of the present paper is to test the validity of the patterns in figure 1

through two-point space–time correlations of u, v and temperature fluctuations.† Emphasis is given to the v-correlations as earlier exploratory measurements with one X-probe on the jet centreline revealed a distinct peak in the v-spectrum when no peak could be discerned in the u-spectrum. On the basis of two-point velocity correlation results, Mumford (1982) indicated that the pattern shown of figure 1 was only one basic structure in the plane jet, another basic structure consisting of roller-like eddies with axes aligned approximately with the direction of the strain associated with the mean velocity gradient. These basic structures could occur in various combinations. The present investigation focuses only on the spanwise structure, the extent of two-dimensionality being considered through spanwise correlations of v. An attempt is also made to estimate the extent of streamwise organization using spectral coherence measurements and to identify the likely spatial origin for these structures.

2. Experimental arrangement and conditions

The experimental facility consists of a variable-speed centrifugal squirrel cage blower which supplies air to a 25 cm × 25 cm × 1.1 m duct leading to a vertical nozzle of contraction ratio 20:1. An aluminium bounding plate of width 25.5 cm and height 28 cm and with a centrally located vertical slit of width $d = 12.7$ mm and of height 25 cm is fixed at the nozzle exit. Two confining horizontal walls (0.7 m wide × 1.1 m long) are located at the upper and lower edges of the aluminium plate. The jet is heated by 1 kW electrical coil elements located immediately downstream of the blower exit.

The velocity fluctuations u (longitudinal x-direction), v (lateral y-direction) in the unheated jet were obtained simultaneously at two locations in the jet using X-probes located in the (x, y)-plane. These probes, built in-house, were designed partly to enable easy mounting of wires and partly to minimize the possibility of interference of the flow by the probe supports, especially in regions where flow reversal becomes important. The hot wires were mounted on separate probes so that replacement of broken wires could be easily effected. The probes could then be mounted on the same assembly (henceforth referred to as an X-probe) with provision for adjusting the configuration of the wires and their separation. The second X-probe is essentially the mirror image of the first probe about the jet centreline.

For the present experiments, 5 μm Pt–10 % Rh Wollaston wires (length ≈ 0.6 mm, separation ≈ 0.6 mm) were used. The wires were cleaned in an ultrasonic bath after etching. The resistances of the wire could be matched to within 1 %. The wires were operated with constant-temperature anemometers (DISA 55M10) at an overheat of 0.8. The four signals from the anemometer bridges were recorded on FM tape (HP3968A) after appropriate signal conditioning. These signals were later digitized using a PDP 11/34 and stored on tape.

The X-probes were calibrated for yaw and velocity at the jet exit. The jet exit velocity was measured using a Pitot-static tube connected to a Furness micromanometer with a resolution of 0.01 mmH_2O. The anemometer voltages and the output voltage from the Furness micromanometer were processed to determine the calibration constants, including the effect inclination of the wires, from least-square fits to hot-wire response equations. For this process, a data-logger consisting of a Hewlett–

† While the two-point correlation approach may, given the inevitable uncertainty (e.g. Townsend 1976) in inferring velocity patterns from correlations, be adequate for this purpose, it does not permit a detailed analysis of the flow field associated with these patterns. A multipoint approach (such as used by Townsend 1979; Mumford 1982) would be better suited for such analysis.

Packard 3497A data acquisition/control unit and a HP-85 desktop computer were used. This facility also ensured satisfactory performance of the hot wires as the wire signals were monitored and processed on the data logger while the experiment was in progress. The X-probes were mounted on separate traversing systems, each with a resolution of 0.01 mm.

All measurements were made in the (x, y)-plane, at $z = 0$ (see figure 1) and a nominal jet exit velocity U_j of 9 m s^{-1} ($R_j \approx 7620$). The two-dimensionality of the flow had been established by distributions of mean velocity, mean temperature, Reynolds stresses and intermittency factor in the (x, z)-plane at different values of y. At the nozzle exit, the boundary layers were laminar with a velocity distribution that closely followed the Blasius profile. Also at this point the momentum thickness was 0.23 mm, the Reynolds number based on this thickness was 140 and the longitudinal r.m.s. velocity about 0.2 % U_j.

A few measurements were made of temperature fluctuations at points symmetrically located on opposite sides of the centreline. For these measurements, the jet was heated to a nominal exit temperature of 25 °C above ambient. The temperature fluctuation θ was measured with 0.63 μm (Pt–10 % Rh) cold wires operated in constant-current (0.1 mA) circuits.

One-dimensional spectra and cross-spectra were directly calculated from discrete Fourier transforms of the time series corresponding to the velocity fluctuations. Using a fast Fourier transform the data were transformed in records basically of 2 min duration. Records up to 7 min duration were used to investigate the long-term periodicity of correlations and when relatively large streamwise separations between the two probes were involved. Auto- and cross-correlations were computed by inverse-Fourier transforming the corresponding spectral densities. The correlation coefficient of velocity fluctuations at two points $\boldsymbol{x}$ and $\boldsymbol{x}+\boldsymbol{r}$ is defined as

$$\rho_{ij}(\boldsymbol{x}, \boldsymbol{x}+\boldsymbol{r}; \tau) = \frac{\overline{u_i(\boldsymbol{x}, t-\tau)\, u_j(\boldsymbol{x}+\boldsymbol{r}, t)}}{u_i'(\boldsymbol{x})\, u_j'(\boldsymbol{x}+\boldsymbol{r})},$$

where a prime denotes an r.m.s. value and subscripts i and j denote the directions of the velocity fluctuations. Subscripts 1 and 2 refer to the x- and y-directions respectively. When $i = j$ (the summation convention on indices is not used), ρ_{ij} is an autocorrelation coefficient. When $i \neq j$, ρ_{ij} is the cross-correlation coefficient.

3. General characteristic features of the flow

Distributions of mean velocity and Reynolds stresses $\overline{u^2}$, $\overline{v^2}$, $\overline{uv}$ indicated approximate self-preservation for $x/d \gtrsim 20$. The growth rate of the velocity half-width L_u, the decay rate of the centreline velocity U_0 and the position of the virtual origin (Antonia *et al.* 1982) differed slightly from the results obtained by others. This is not surprising since these quantities have been shown to be influenced by initial conditions, nozzle geometry, aspect ratio and room turbulence (see Krothapalli, Baganoff & Karamcheti 1981).

Flow reversal in the outer regions of circular and plane jets into still air has been established in the literature (Kotsovinos 1975; Lau, Morris & Fisher 1979; Moallemi & Goldschmidt 1981; Antonia *et al.* 1983). In the present investigation, flow reversal was detected by placing a cold wire upstream of and orthogonal to the plane of the hot wires in the X-probe. Detection of the hot wires' thermal wakes was first noted at $\eta = y/L_u \approx 1$. As fluctuations u and v are likely to be in error beyond this region of the flow, data presented in the following sections are only up to $\eta \approx 1.2$.

4. Spectra and space correlations at zero time delay

Spectral densities of u, v on the jet centreline revealed large peaks at $x/d = 4$. The amplitude of these peaks decreases with increasing x/d. In particular, the peak in the u-spectrum was no longer evident at $x/d = 14$, but the peak in the v-spectrum was present up to $x/d = 60$, the largest value considered here.† For $x/d < 14$, peaks in the u- and v-spectra occurred at the same frequency. It should be noted that, while spectra of velocity fluctuations measured at one point in space may fail to detect quasiperiodicity of the flow, two-point statistics, such as the coherence Coh_{11} between Fourier components of u obtained at two different locations in space, could be a more effective detector. In this context, Keffer (1979) noted that, in the turbulent wake of a heated cylinder, the temperature spectrum at $x/d = 40$ (d is the cylinder diameter) did not exhibit a peak at the vortex-shedding frequency, but the coherence between temperature fluctuations measured at $x/d = 6$ and $x/d = 40$ did exhibit a significant peak at the Strouhal frequency.

Krothapalli *et al.* (1981) presented autocorrelations and spectra of u on the centreline of a plane jet over the range $2 \leqslant x/d \leqslant 20$. As for the present investigation, the boundary layers at the nozzle exit were laminar. Strong periodicity was visible in the time record of u and in the autocorrelation function of u for $x/d < 4$. The periodicity could be recognized up to $x/d \approx 10$. At $x/d = 20$ the autocorrelation function did not show any sign of periodicity. While these observations are similar to those reported for the present experiments, Krothapalli *et al.* mentioned that fluctuations v and w exhibited features similar to u and concluded that discrete frequencies appeared only in the initial stages of transition between laminar and turbulent flow. This conclusion is not supported by the present measurements since, as mentioned previously, a peak exists in the v spectrum at least up to $x/d = 60$.

As expected, the frequency f_p at which the peak in the v-spectrum occurs also corresponds to the time delay at which the one-point autocorrelation coefficient ρ_{22} exhibits a second maximum (the first maximum is at $\tau = 0$). This frequency is the average frequency of occurrence of the vortical structures, to be discussed in more detail later. When f_p is normalized by L_u and U_0, an approximately constant value of $f_p L_u/U_0$ is evident (figure 2) for $x/d \gtrsim 20$. This seems consistent with the observed approximate self-preservation, for $x/d \gtrsim 20$, of distributions pertaining to both mean and fluctuating velocity and temperature fields. The constant value (≈ 0.11) of $f_p L_u/U_0$ is in good agreement with the value obtained by Cervantes & Goldschmidt (1981) (the constancy extended up to $x/d \approx 90$ in their experiment). As in Cervantes & Goldschmidt's experiment, the magnitude of f_p was independent of y for any particular value of x.

The coherence between v-fluctuations obtained at $\eta = \pm 0.5$ and $\eta = \pm 1.0$ at $x/d = 40$ show maxima at the frequency at which the v-spectrum exhibits a peak. Spectral densities of v at these η are in good agreement with each other, providing support for the symmetry of the flow about the jet centreline.

Autocorrelation coefficients ρ_{11} and ρ_{22} at zero time delay obtained with X-probes symmetrical about the centreline are plotted in figure 3 as a function of $|\eta|$ (the separation between probes is equal to $2|\eta|$). The behaviour of ρ_{11} is similar to that already available in the literature. The distribution, representing data at several stations, obtained by Cervantes & Goldschmidt (1981) differs slightly from the present distribution exhibiting a minimum at $|\eta| \approx 0.65$ instead of $|\eta| = 0.5$. The

† Papailiou & Lykoudis (1974) refer to measurements on the centreline of a cylinder wake by Bevilaqua, who found that, whereas u appeared to be random, v showed a pronounced periodicity.

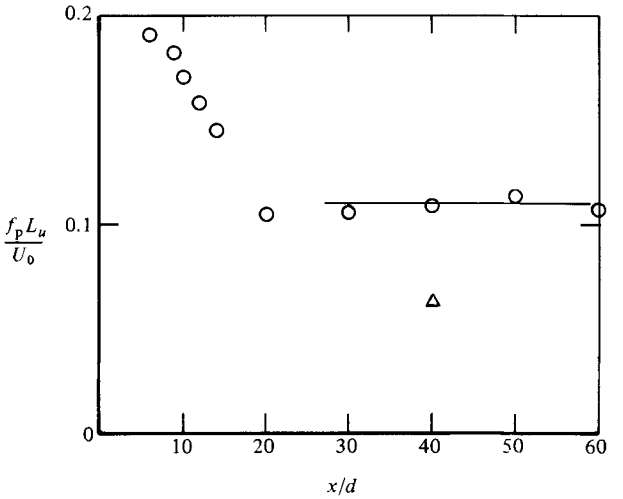

FIGURE 2. Variation on centreline of frequency f_p normalized by L_u and U_0: ○, present – based on peak frequency of v-spectrum; ——, Cervantes & Goldschmidt (1981); △, Goldschmidt & Bradshaw (1973).

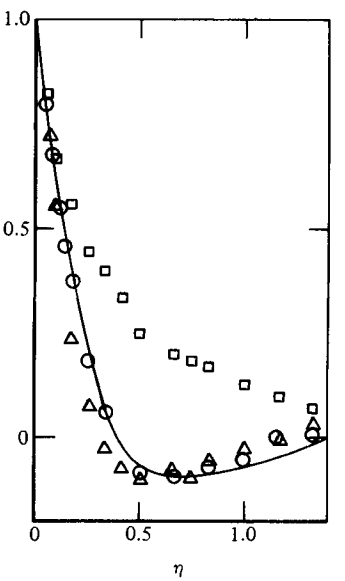

FIGURE 3. Autocorrelation coefficients, at zero time delay, between u- or v- or temperature fluctuations on opposite points of the centreline at $x/d = 40$. Present: △, ρ_{11}; □, ρ_{22}; ○, $\rho_{\theta_1\theta_2}$. Cervantes & Goldschmidt (1981): ——, ρ_{11}.

rate of change of ρ_{22} with $|\eta|$ seems to slow down for $|\eta| \approx 0.5$, the position at which ρ_{11} is minimum. Values of the autocorrelation coefficient $\rho_{\theta_1\theta_2}$ at zero time delay of temperature fluctuations obtained at points symmetrical with respect to the centreline at $x/d = 40$, have been included in figure 3. This coefficient becomes negative at $\eta \approx 0.35$, in reasonable agreement with the behaviour exhibited by ρ_{11}.

Correlation coefficients and maximum coherences between u- and v-fluctuations were also obtained with one X-probe fixed at $\eta = -1$ and the other traversed across the jet. The maximum correlation coefficient ρ_{11} (figure 4) occurs at $\tau = 0$, as does ρ_{22}, and becomes negative at $\eta \approx 0$. The coefficient ρ_{22} remains positive and is

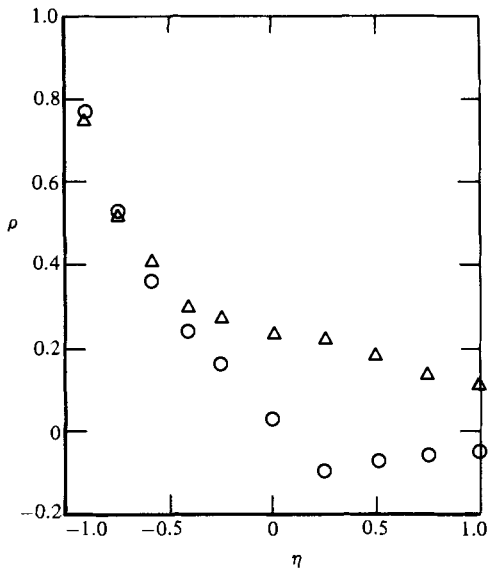

FIGURE 4

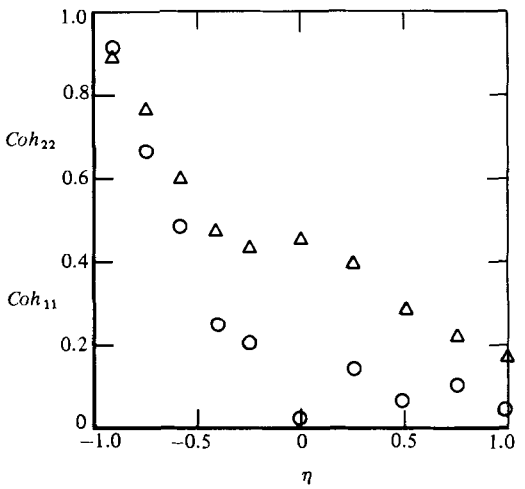

FIGURE 5

FIGURE 4. Autocorrelation coefficients, at zero time delay, between u- or v-fluctuations with one X-probe fixed at $\eta = -1$ ($x/d = 40$): ○, ρ_{11}; △, ρ_{22}.

FIGURE 5. Maximum coherences between u- and v-fluctuations with one X-probe fixed at $\eta = -1$ ($x/d = 40$): ○, Coh_{11}; △, Coh_{22}.

significantly larger than ρ_{11} for $\eta \gtrsim -0.5$. The difference between ρ_{11} and ρ_{22} is reflected in the difference (figure 5) between the maximum values of Coh_{11} and Coh_{22}. The maximum values of Coh_{22} occur at $f = f_p$, independent of η, and remain significant to $\eta = +1$.

An idea of the lateral scale y_s of the structures can be obtained by integrating the ρ_{22} distribution (figure 4) with respect to y. The resulting integral scale

$$L_y = \int_0^\infty \rho_{22} \mathrm{d}y = 0.65 L_u.$$

Had ρ_{11} been used instead of ρ_{22}, this scale would be reduced to $0.37 L_u$.

Correlations of u and v, using two X-probes, were also measured in the spanwise direction. The relative behaviour of ρ_{22} and ρ_{11} was qualitatively similar to that found for lateral separations (figure 3). In particular ρ_{22} was always maximum at zero time delay and remained positive at the largest separation ($\Delta z \approx 2.5 L_u$) considered for $\eta = 0.5$. Like the spanwise correlations of u measured by Oler & Goldschmidt (1981) and Mumford (1982), $\rho_{11}(\Delta z)$ exhibited a negative lobe. There has been much speculation as to the reason for this negative contribution: Oler & Goldschmidt gave more weight to the flow-visualization results (Moallemi & Goldschmidt 1981) than to their $\rho_{11}(\Delta z)$ distribution, which implied a limited two-dimensionality of the vortex street. As $\rho_{11}(\Delta z)$ should receive contributions by other structures, such as inclined roller eddies with circulation in the (x, z)-plane, it is likely that $\rho_{22}(\Delta z)$ is a better indicator than $\rho_{11}(\Delta z)$ of the two-dimensionality of the spanwise structures. This is supported by comparison of integral lengthscales obtained using ρ_{22} and ρ_{11}.† The

† It is also in agreement with the observation in a mixing layer by Wygnanski *et al.* (1979).

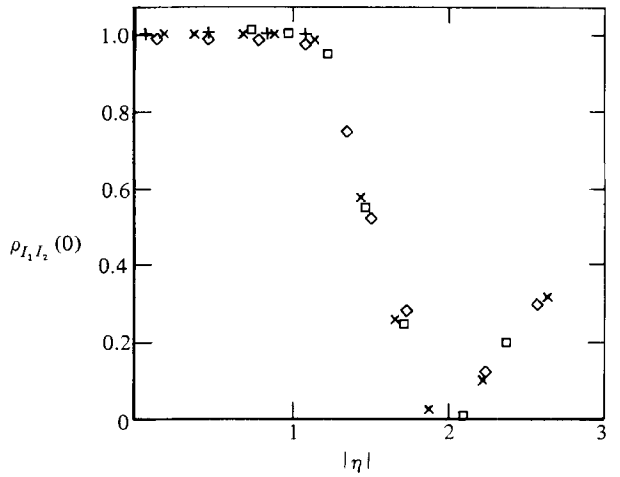

FIGURE 6. Autocorrelation coefficients, at zero time delay, of intermittency functions I based on temperature fluctuations. The cold wires are symmetrically located with respect to the centreline. □, $x/d = 20$; ×, 30; ◇, 40; +, 50.

integral scale $L_z\left(=\int_0^\infty \rho_{22}\,\mathrm{d}z\right)$ is estimated to be equal to about $0.49L_u$ at $\eta = +0.5$. Had $\rho_{11}(\Delta z)$ been used, a value of $0.26L_u$ would have resulted for L_z. The integral lengthscale L_x in the x-direction can be inferred from the time autocorrelations for u or v. For the present experiment at $\eta = 0.5$, $L_x/L_u \approx 0.64$ and 0.37 when u and v are used respectively. These ratios were found to be relatively insensitive to the spanwise location of the probe. Using u, the ratio $L_x/L_z = 2.5$ compares favourably with values of 2.3 and 2.0 obtained by Oler & Goldschmidt (1981) and Everitt & Robins (1978). When v is used, the present ratio L_x/L_z is about 0.75.

Correlation coefficients $\rho_{I_1 I_2}$† of the intermittency function I, determined at points symmetrical about the centreline, are shown in figure 6. One constraint on the shape of the correlation is the requirement that the correlation coefficient must be unity when the temperature sensors are either near the centreline or in ambient temperature fluid. Associated with the highly contorted hot/cold interface is the high probability of finding no correlation between interfaces on opposite sides of and at a sufficiently large distance from the centreline. The behaviour of $\rho_{I_1 I_2}$ is similar to that obtained by Wygnanski & Gutmark (1971) and Moum *et al.* (1979). In the light of all the results presented in this section, it is evident that the conclusion reached by these investigators with regard to independence of boundary motion is not incompatible with the asymmetric vortex-street pattern of figure 1.

The possibility of wholesale flapping (as against apparent flapping associated with the pattern of figure 1) can be considered in the context of the flapping amplitude estimated by Goldschmidt & Bradshaw (1973). The estimate is based on the assumption of a sinusoidal bodily displacement ϵ of the mean velocity profile from its mean location

$$\epsilon = \epsilon_{\mathrm{m}} \sin 2\pi\tau f_{\mathrm{p}},$$

† The intermittency function I was derived from the temperature fluctuation using the method outlined by Sreenivasan, Britz & Antonia (1977). Subscripts 1 and 2 refer to the points at which temperature fluctuations are measured.

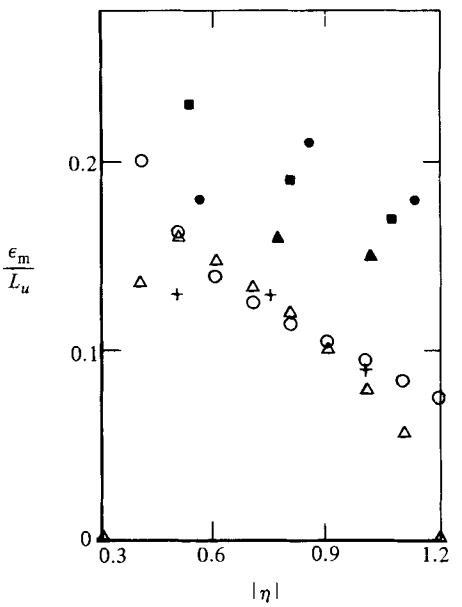

FIGURE 7. Amplitude of flapping, obtained from two-point autocorrelations of u- and v-fluctuations at $x/d = 40$. The X-probes are symmetrically located with respect to the centreline. Present results: ○, based on v; △, u. Cervantes & Goldschmidt (1981) based on u: ▲, $x/d = 40$; ■, 60; ●, 80. Goldschmidt & Bradshaw (1973): +, based on u.

where f_p^{-1} is identified here with the period of flapping and $\frac{1}{2}\epsilon_m$ is the maximum amplitude of flapping. Rough approximations to the non-random components of u or v can be written as

$$\alpha \approx \frac{\partial \overline{U}}{\partial y}\epsilon \quad (\alpha \equiv u \text{ or } v)$$

At $\tau = 0$, the normalized amplitude ϵ_m/L_u can be expressed as

$$\frac{\epsilon_m}{L_u} \approx \frac{[2|\rho_{ij}(0)|]^{\frac{1}{2}}}{|f'|}\frac{(\overline{\alpha^2})^{\frac{1}{2}}}{U_0},$$

where $f \equiv \overline{U}/U_0$ and the prime denotes differentiation with respect to η. Resulting distributions, corresponding to ρ_{11} and ρ_{22}, are plotted in figure 7 for $\eta > 0.3$ (ρ_{11} becomes negative at $\eta \simeq 0.3$, cf. figure 3). There is a range of η for which the amplitude is independent of whether u or v is used. While the present amplitude is in closer agreement with the measurements of Goldschmidt & Bradshaw (1973) than with those of Cervantes & Goldschmidt (1981), there is no indication in figure 7 of a constant value for ϵ_m/L_u, and consequently little support for the concept of a sinusoidal bodily displacement of the velocity profile as might be associated with a wholesale flapping of the jet.

5. Convection velocities

Space–time correlations of velocity fluctuations have been used extensively to determine convection velocities in different turbulent flows. Convection velocities are estimated here using space–time correlations of u and v. As in the case of Goldschmidt

et al. (1981), both broadband and wavenumber-dependent convection velocities are considered. For the former case, the convection velocity is defined as the ratio of the longitudinal spacing Δx between two X-probes and the time delay $\tau_{\max}$ at which correlation coefficients ρ_{11} and ρ_{22} are maximum viz

$$U_c = \frac{\Delta x}{\tau_{\max}}. \tag{1}$$

Strictly (1) should be obtained in the limit as $\Delta x \to 0$. In practice, a finite separation is required (e.g. Goldschmidt, Young & Ott 1981; Davies & Mercer 1973) to avoid possible interference with the flow by the upstream probe. The present value of Δx (≈ 20 mm) was such that the thermal wakes from the upstream hot wires did not interfere with the downstream X-probes. For this separation, the statistics of u and v obtained from the downstream X-probe were unaffected by the presence of the upstream X-probe. To provide adequate resolution for the determination of $\tau_{\max}$, the analogue voltages corresponding to u and v were digitized at a sampling frequency of the order of the Kolmogorov frequency (≈ 3.4 kHz) at the jet centreline. The autocorrelation coefficients ρ_{11} and ρ_{22} were maximum at the same value of $\tau_{\max}$ so that no distinction is made here between broadband convection velocities determined from either u or v. The ratio U_c/U_0 ($\leqslant 1$) is in good agreement with that obtained, using u, by Goldschmidt *et al.* (1981).

The frequency-dependent phase velocity U_p can be inferred from the phase angle ϕ_{ij}† and frequency ω via the relation

$$U_p = \Delta x \frac{\omega}{\phi_{ij}}, \tag{2}$$

where ϕ_{ij} is in radians. The ratio ϕ_{ij}/ω could be identified with the time of flight of the eddy associated with frequency ω over the distance Δx. Distributions of ϕ_{11} and ϕ_{22} showed a linear increase with frequency up to f_p, suggesting a velocity approximately independent of frequency. The phase velocity based on u is larger than that based on v but, except at $\eta = 0$, is consistently smaller than U_c.

Cervantes & Goldschmidt (1981) obtained a 'convection velocity of flapping' U_f by determining $\tau_{\max}$ for ρ_{11} when single hot wires with a small Δx displacement were symmetrically placed on opposite sides of the centreline. A similar approach was used here, although v was preferred to u in view of the relatively large values of Coh_{22} in relation to Coh_{11}. The agreement (figure 8) between this velocity of flapping and the phase velocity U_p tends to support further the notion that the flapping motion is more likely to be associated with organized structures such as sketched in figure 1 than with a wholesale flapping of the jet. The variation of U_p or U_f with η tends to indicate that some straining of the structures may occur as they are convected downstream.

6. Space–time correlations

Space–time correlation coefficients of u- and v-fluctuations obtained on opposite sides ($\eta = \pm 0.5$) of the centreline at $x/d = 40$‡ are shown in figure 9. The one-point cross-correlation coefficients between u and v are of opposite sign and of approximately equal magnitude, as required by symmetry with respect to the centreline. The two-point coefficient ρ_{11} exhibits a negative minimum at $\tau = 0$, with positive maxima

† Note that $\tan \phi_{ij}$ is the ratio of the quadrature to the cospectrum of fluctuations u_i and u_j.

‡ Results for $x/d = 20$ and 30 and $\eta = \pm 0.5$ are identical with those in figure 9 and are not shown.

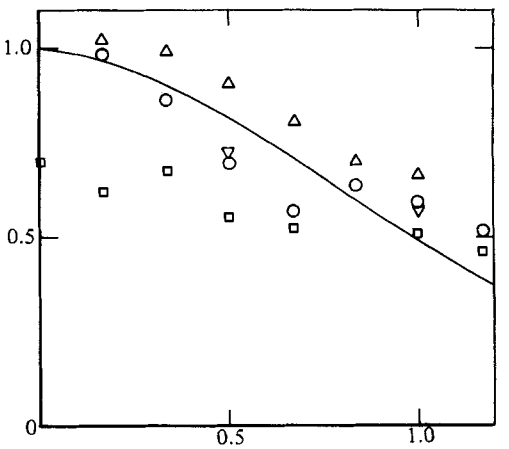

FIGURE 8. Convection velocities normalized by U_0 ($x/d = 40$): △, U_c, using the time delay τ_{max} at which two-point auto-correlations of u or v are maximum; ○, using phase velocity U_p based on u; □, using phase velocity U_p based on v; ——, $\bar{U}/U_0$; ▽, U_f/U_0.

of smaller magnitude at $|\tau| U_0/L_u \approx 4$. In contrast, ρ_{22} has a positive maximum at $\tau = 0$ and exhibits distinct minima at $|\tau_{min}| U_0/L_u \approx 3$. These minima are followed or preceded by secondary maxima of smaller magnitude at $|\tau_{max}| U_0/L_u \approx 7.5$. Corresponding to these maxima are hardly recognizable minima in ρ_{11} at $|\tau| U_0/L_u \approx 8.5$. The uncertainty ($\pm 1.5$) in this location is somewhat larger than that for the secondary maxima in ρ_{22}.

An approximate idea of the streamwise extent (size) and wavelength (distance between arrival of successive structures) of the organized motion can be inferred from the locations of the first minimum and second maximum of ρ_{22} (or ρ_{11}, although the uncertainty would be greater in this case) and the convection velocity of the motion. The streamwise extent suggested by ρ_{22} (figure 9) is given by

$$\frac{x_s}{L_u} = \left(\frac{\tau_{min} U_0}{L_u}\right)\frac{U_f}{U_0} \approx 2.2$$

if U_f ($\approx 0.73 U_0$ for $\eta = \pm 0.5$) is identified with the convection velocity of this motion. An estimate for the streamwise wavelength λ_s of the structures would be

$$\frac{\lambda_s}{L_u} = \left(\frac{\tau_{max} U_0}{L_u}\right)\frac{U_f}{U_0} \approx 5.5$$

(i.e. $\lambda_s \approx 0.6x$† for $20 < x/d < 60$ or $\lambda_s \approx 24d$ at $x/d = 40$). Oler & Goldschmidt's (1981) isocorrelation contours of ρ_{11} were interpreted to indicate a measurable flow organization over a streamwise distance of about $25d$ at $x/d = 30$. Included in figure 9 are the two-point correlation coefficients ρ_{12} and ρ_{21}. Apart from a small phase shift (ρ_{12} is minimum at a slightly negative τ while ρ_{21} is maximum at a slightly positive τ), ρ_{12} and ρ_{21} closely reflect the behaviour of ρ_{11} and ρ_{22} respectively. The relative behaviour of all two-point coefficients is consistent with the structures of figure 1. The behaviour, with respect to time, of the correlation ρ_{22} in the spanwise direction (figure 10) is fully consistent with that exhibited with the lateral correlation:

† Note in the present experiment, for $x/d \gtrsim 20$, $L_u/d = 0.104\,(x/d + 5)$.

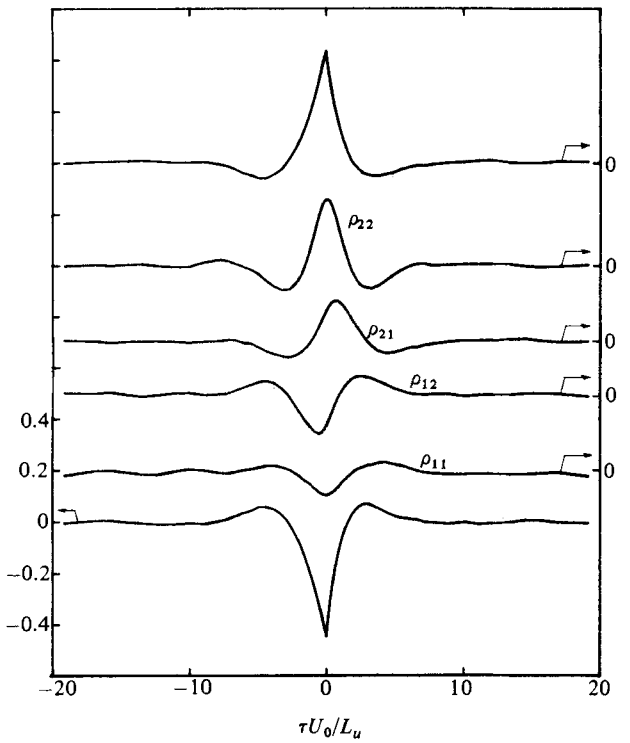

FIGURE 9. Auto- and cross-correlation coefficients of u- and v-fluctuations at $x/d = 40$. The X-probes are at $\eta = \pm 0.5$. The bottom and top traces correspond to one-point cross-correlations between u and v at $\eta = -0.5$ and $\eta = +0.5$ respectively.

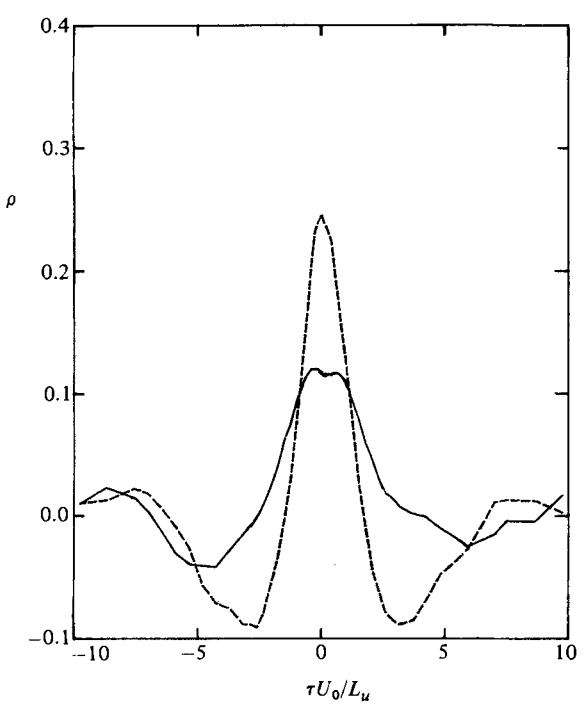

FIGURE 10. Autocorrelation coefficients of u- and v-fluctuations with X-probes at $x/d = 40$, $\eta = +0.5$ and a spanwise separation of $0.5L_u$. On of the X-probes is at $z = 0$. ——, $\rho_{11}(0)$; – –, $\rho_{22}(0)$.

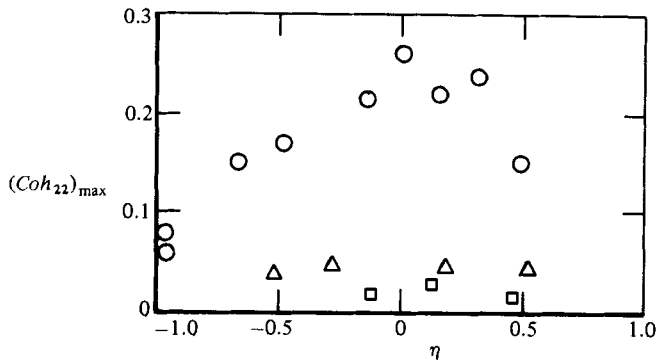

FIGURE 11. Maximum coherence associated with two-point autocorrelations of v. One X-probe is fixed at $x/d = 40$ and $\eta = +0.5$. The other is moved to different values of x/d and η. ○, $x/d = 20$; △, 14; □, 8.

estimates of x_s and λ_s do not depend on whether lateral or spanwise separations are used when forming the correlation. For the separation used in figure 10, $\rho_{11}(0)$ is positive but only about half the magnitude of $\rho_{22}(0)$.

To confirm the spatial extent of the organized motion inferred from two-point space–time correlations at one value of x/d, space–time correlations were measured at two points separated in both x- and y-directions. The maximum coherence between v-fluctuations obtained with one of the X-probes fixed ($\eta = +0.5$) at $x/d = 40$ and the other one at different lateral positions for three values of x/d is shown in figure 11. At $x/d = 20$, the coherence is remarkably large (≈ 0.25) near the centreline. For comparison, the maximum value of Coh_{11} is smaller than 0.05 at $x/d = 20$, underlining the attractiveness of using v instead of u. It should be noted that the maximum coherence occurs at neither the frequency (≈ 6 Hz) corresponding to the peak in the v-spectrum at $x/d = 40$ nor that (≈ 15 Hz) at $x/d = 20$, but at some intermediate frequency (≈ 9 Hz). This result is consistent with the growth of the structures as they are convected downstream.

A rough estimate of the lateral size of the structures can be inferred from the onset of flow reversal. As noted previously this is first observed at about L_u. The lateral size y_s of the structure is thus of order L_u. Another estimate for y_s can be inferred by integrating the maximum coherence (figure 5) between v-fluctuations in the lateral direction. The integration yields $0.97L_u$ for y_s. An approximate estimate for the spanwise extent z_s was obtained by integrating the maximum coherence of v-fluctuations in the z-direction. The integration yielded $0.72L_u$ for z_s. It should be noted, however, that this estimate, while more realistic than one based on ρ_{22}, may be a pessimistic indicator of the degree of structural two-dimensionality.

Space–time correlations of u- and v-fluctuations on opposite sides of the centreline were extended to small values of x/d in an attempt to establish the nature of the flow in the interaction region and its possible relationship to that in the self-preserving regions of the jet. At $x/d = 6$, the two-point coefficients ρ_{11} and ρ_{22} (figure 12) with the X-probes located at $y/d = \pm 1.18$ exhibit a positive maximum and negative minimum respectively at $\tau = 0$. For ρ_{22}, this minimum is flanked for positive and negative values of τ, by positive maxima of smaller amplitude. This pattern is subsequently repeated for both positive and negative τ with unmistakable periodicity. The sign and relative behaviour of ρ_{11} and ρ_{22} are consistent with the existence of symmetric counter-rotating structures in the opposite mixing layers. The behaviour

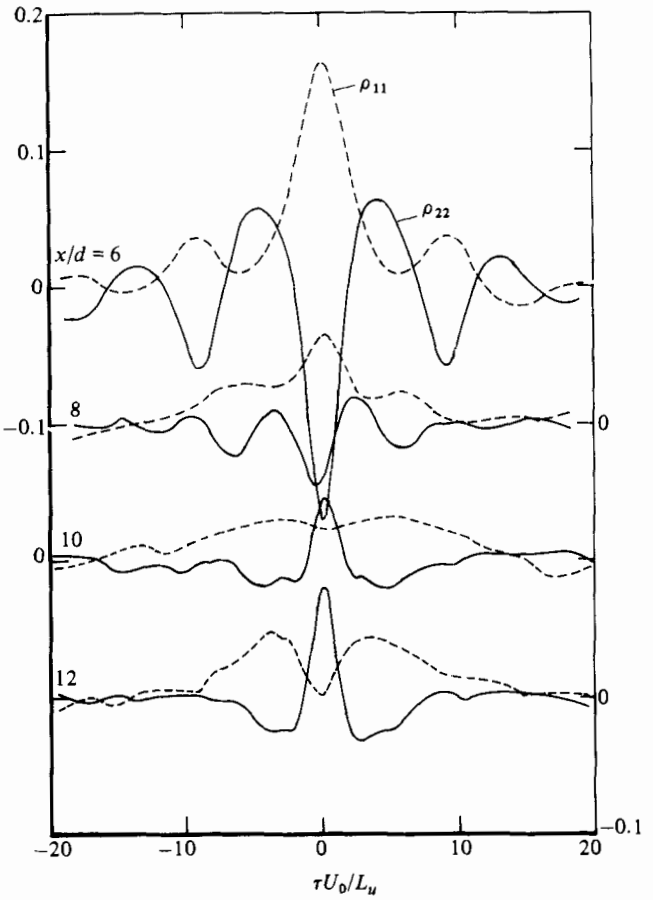

FIGURE 12. Autocorrelation coefficients of u- and v-fluctuations in the interaction region. The X-probes are at $y = \pm 1.18d$.

of ρ_{11} and ρ_{22} at $x/d = 4$† (not shown in figure 12) is similar to that for $x/d = 6$ except for much larger values of the correlations (at $\tau = 0$) and maximum coherence. In the case of v, the maximum coherence Coh_{22} decreases from 0.5 at $x/d = 4$ to 0.2 at $x/d = 6$, with the X-probes at $y/d = \pm 1.18$. With a further increase in x/d, this coherence begins to increase and the pattern of the space–time correlation coefficients at $x/d = 10$ differs appreciably from that at $x/d = 8$. At $x/d = 10$, ρ_{11} is relatively small at $\tau = 0$ and exhibits weak local maxima at $|\tau| U_0/L_u \approx 4$. The coefficient ρ_{22} is positive at $\tau = 0$ and exhibits weak minima at $|\tau| U_0/L_u \approx 4$. This relative behaviour of ρ_{11} and ρ_{22} is characteristic of that in the self-preserving region (figure 9). The tendency for ρ_{11} to develop a negative minimum at $\tau = 0$ is evident at $x/d = 12$. The onset of the asymmetry thus occurs in this region.

Both symmetric and asymmetric modes of vortex growth with respect to the centreline of plane jets have been noted by several prior studies. Most of Brown's (1935) smoke photographs of plane jets subjected to external acoustic excitation showed alternating vortical structures but symmetric vortex patterns can be seen in a few. In a study of the stability and transition of a plane jet, Sato (1960) detected both symmetric and asymmetric, with respect to the centreline, u-fluctuations. Using

† The potential core nominally ends at $x/d \approx 5$.

hydrogen-bubble flow visualization over the range $1860 < R_j < 10800$, Rockwell & Niccolls (1972) found that the vortex growth and coalescence in a plane jet can be either symmetric or asymmetric. The symmetric and asymmetric arrangements lead to varicose and sinuous modes of instability respectively. In their study of initial conditions on the near field of a plane jet, Oseberg & Kline (1971) noted that, while asymmetric modes were occasionally observed, the vortex arrays were primarily symmetric. Observations, by Beavers & Wilson (1970), of the growth of vortices in the vortex streets bounding the jet emerging from a sharp-edged two-dimensional slit ($500 \lesssim R_j \lesssim 3000$) indicated symmetric patterns of vortex pairs. Wygnanski & Gutmark (1971) noted that the intermittency traces obtained at $x/d \approx 0.5$ from two hot wires symmetrically placed about the centreline of their plane jet ($R_j \approx 3 \times 10^4$) were perfectly matched. The matching was attributed to the rolling up of the first vortex near the exit of the jet. Weir & Bradshaw (1975) found that the initial region of two turbulent plane jets associated with the exit planes of two-dimensional contractions exhibited a flapping motion with a frequency independent of x, up to $x/d = 12$. This motion was inferred from the negative correlations in single hot-wire outputs obtained at locations ($\pm\frac{1}{2}d$) in opposite mixing layers. These authors suggested that this flapping or resonant oscillation is a universal feature of plane jets and speculated that it may possibly be the ancestor of the flapping motion suggested by Goldschmidt & Bradshaw (1973). The present measurements were made with a contraction similar in shape to that used by Weir & Bradshaw (1975) for their 30 in. × 5 in. jet but the present Reynolds number is one order of magnitude smaller than that ($R_j = O(10^5)$) of Weir & Bradshaw. These authors interpreted the negative correlation as due to the bodily displacement or flapping of the jet and estimated an amplitude of the flapping to be about $0.031d$. Although the possibility that the negative correlation may have been associated with an asymmetric vortex street was not considered, it would seem unlikely that the frequency of these vortices was independent of x. The present measurements and other previously cited experimental results in the initial region of a plane jet are in conflict with the suggestion that flapping is a universal feature of this region. Also, it is unlikely that flapping occurs only at large Reynolds numbers; in Uberoi & Singh's (1975) experiment, where a lateral motion of the jet boundaries was evident, the jet-exit Reynolds number was only about 200.

7. Conclusions and final discussion

The correlations and coherences between longitudinal and/or lateral velocity fluctuations measured at two points in space, satisfy the spatial relations for the instantaneous velocity field associated with quasiperiodic counter-rotating structures alternating on opposite sides of the centreline in the self-preserving region of a turbulent plane jet, as suggested by Oler & Goldschmidt (1981). Temperature correlations also confirm the presence of these structures. The estimated streamwise extent ($\approx 2.2L_u$) of the structures is at least two to three times as large as the lateral ($\approx L_u$) and spanwise ($\approx 0.7L_u$) extents.

The frequency of occurrence of the structures is unambiguously inferred from spectra of v-fluctuations and scales on the half-width and the centreline mean velocity in the self-preserving region of the jet. The magnitude of this frequency is in good agreement with that obtained by Cervantes & Goldschmidt (1981). The apparent flapping is associated with the quasiperiodic passage of the structures. It is not caused by a bulk displacement of the mean velocity profile. Further, it is not incompatible

with the suggestion, made by several investigators, that the opposite jet boundaries move independently of each other.

The extent of streamwise organization of the structures is reflected in measurements of the coherence of v-fluctuations obtained, with relatively large streamwise separations, on either opposite sides or on the same side of the centreline. The asymmetry, with respect to the centreline, of the structures is no longer observed for x/d smaller than about 10. Near the jet exit plane, similar structures are observed in the mixing layers. These structures are strongly symmetric with respect to the centreline. The symmetry disappears downstream of where the mixing layers merge.

Cervantes (1981) suggested that a waveguide model might account for some of the observations by Cervantes & Goldschmidt (1981). In particular, the model predicts a sinuous mode (with larger amplification rates than the varicose mode) which could account for the out-of-phase u-fluctuations on opposite sides of the centreline in the self-preserving region. The tendency for this sinuous mode to reach maximum growth further downstream was noted to be consistent with the relatively low and decreasing (with streamwise distance) frequencies associated with the asymmetric structures. Cervantes presented an overall (and by necessity rather simplified) view of the structural development of a turbulent plane jet. The initial mixing layers interact downstream of the end of the potential core, the result of this interaction accounting, in as yet unexplained fashion, for the asymmetry in the self-preserving region.

The present investigation, while confirming the nature of the organized motion proposed by Oler & Goldschmidt (1981), reveals that the structures are established well downstream of the nominal merging point of the mixing layers but upstream of the onset of self-preservation. It is possible that the interaction of structures from the opposite mixing layers results in their destruction (e.g. figure 12) and that new structures are formed soon after the destruction is completed. The formation and possible locking mechanism for the structures in the interaction region require further investigation. Another interesting aspect that should be investigated is the effect of Reynolds number on the organized motion. In this context, Crow & Champagne (1971) showed how the pattern of organized motion in the mixing region of a circular jet changed with Reynolds number, the surface ripples tending to disappear at high Reynolds numbers.

It is important to determine what contributions to momentum and heat transfer rates are made by the asymmetric structures considered here and by other structures, such as the inclined rollers with circulation in the (x, y)-plane as considered by Mumford (1982). This may entail an experimental set-up capable of focusing on one or more features of the structures. The use of temperature as a passive marker of the flow and the combination of an X-probe with a rake of cold wires may help in this regard.

The support of the Australian Research Grants Scheme is gratefully acknowledged. We are also grateful to Mr M. J. Watts for his contribution to the measurements of temperature correlations.

REFERENCES

Antonia, R. A., Browne, L. W. B., Chambers, A. J. & Rajagopalan, S. 1983 Budget of the temperature variance in a turbulent plant jet. *Int. J. Heat Mass Transfer.* **26**, 41–48.

Beavers, G. S. & Wilson, T. A. 1970 Vortex growth in jets. *J. Fluid Mech.* **44**, 97–112.

Bradbury, L. J. S. 1965 The structure of a self-preserving turbulent plane jet. *J. Fluid Mech.*, **23**, 31–64.

BROWN, G. B. 1935 On vortex motion in gaseous jets and the origin of their sensitivity to sound. *Proc. Phys. Soc.* **47**, 703–732.

CERVANTES, J. G. 1981 The flapping motion of a turbulent plane jet: a workable relationship to wave-guide theory. In *Unsteady Turbulent Shear Flows* (ed. R. Michel, J. Cousteix & R. Houdeville), pp. 412–424. Springer.

CERVANTES DE GORTARI, J. & GOLDSCHMIDT, V. W. 1981 The apparent flapping motion of a turbulent plane jet – further experimental results. *Trans. ASME* I: *J. Fluids Engng* **103**, 119–126.

CROW, S. C. & CHAMPAGNE, F. H. 1971 Orderly structure in jet turbulence. *J. Fluid Mech.* **48**, 547–591.

DAVIES, P. O. A. L. & MERCER, C. A. 1973 Phase velocity measurements using the cross power spectrum. *Inst. of Measurement & Control Conf. Proc.* pp. 37–45.

EVERITT, K. W. & ROBINS, A. G. 1978 The development and structure of turbulent plane jets. *J. Fluid Mech.* **88**, 563–583.

GOLDSCHMIDT, V. W. & BRADSHAW, P. 1973 Flapping of a plane jet. *Phys. Fluids* **16**, 354–355.

GOLDSCHMIDT, V. W., YOUNG, M. F. & OTT, E. S. 1981 Turbulent convective velocities (broadband and wavenumber dependent) in a plane jet. *J. Fluid Mech.* **105**, 327–345.

GRANT, H. L. 1958 The large eddies of turbulent motion. *J. Fluid Mech.* **4**, 149–190.

GUTMARK, E. & WYGNANSKI, I. 1976 The planar turbulent jet. *J. Fluid Mech.* **73**, 465–495.

KEFFER, J. F. 1979 Measurement of spanwise distribution of turbulent structures. In *Proc. Dynamic Flow Conf.* 1978 *on Dynamic Measurements in Unsteady Flows, Marseille–Baltimore* (ed. L. S. G. Kovasznay, A. Favre, B. Buchhave, L. Fulachier & B. W. Hansen), pp. 231–248.

KOTSOVINOS, N. E. 1975 A study of the entrainment and turbulence in a plane buoyant jet. Ph.D. thesis, California Institute of Technology.

KROTHAPALLI, A., BAGANOFF, D. & KARAMCHETI, K. 1981 On the mixing of a rectangular jet. *J. Fluid Mech.* **107**, 201–220.

LAU, J. C., MORRIS, P. J. & FISHER, M. J. 1979 Measurements in subsonic and supersonic free jets using a laser velocimeter. *J. Fluid Mech.* **93**, 1–27.

LIST, E. J. 1982 Turbulent jets and plumes. *Ann. Rev. Fluid Mech.* **14**, 189–212.

MOALLEMI, M. K. & GOLDSCHMIDT, V. W. 1981 Smoke wire visualization of the external region of a two-dimensional jet. In *Proc. 7th Biennial Symp. on Turbulence, University of Missouri–Rolla*, pp. 42-1–42-10.

MOUM, J. N., KAWALL, J. G. & KEFFER, J. F. 1979 Structural features of the plane turbulent jet. *Phys. Fluids* **22**, 1240–1244.

MUMFORD, J. C. 1982 The structure of the large eddies in fully developed turbulent shear flows. Part 1. The plane jet. *J. Fluid Mech.* **118**, 241–268.

OLER, J. W. 1980 Coherent structures in the similarity region of a two-dimensional turbulent jet: a vortex street. Ph.D. thesis, Purdue University.

OLER, J. W. & GOLDSCHMIDT, V. W. 1981 Coherent structures in the similarity region of two-dimensional turbulent jets. In *Proc. 3rd Symp. on Turbulent Shear Flows, University of California at Davis*, pp. 11.1–11.6.

OLER, J. W. & GOLDSCHMIDT, V. W. 1982 A vortex-street model of the flow in the similarity region of a two-dimensional free turbulent jet. *J. Fluid Mech.* **123**, 523–535.

OSEBERG, O. K. & KLINE, S. J. 1971 The near field of a plane jet with several initial conditions. *Report* MD-28, *Dept Mech. Engng, Stanford University.*

PAPAILIOU, D. D. & LYKOUDIS, P. S. 1974 Turbulent vortex streets and the entrainment mechanism of the turbulent wake. *J. Fluid Mech.* **62**, 11–31.

ROCKWELL, D. O. & NICCOLLS, W. O. 1972 Natural breakdown of planar jets. *Trans ASME* D: *J. Basic Engng* **94**, 720–730.

SATO, H. 1960 The stability and transition of a two-dimensional jet. *J. Fluid Mech.* **7**, 53–80.

SREENIVASAN, K. R., BRITZ, D. & ANTONIA, R. A. 1977 On the accuracy of determining high-order moments of turbulent fluctuations. *Rep.* T.N. – FM10, *Dept Mech Engng, University of Newcastle, N.S.W.*

TOWNSEND, A. A. 1976 *The Structure of Turbulent Shear Flow*, 2nd edn. Cambridge University Press.

TOWNSEND, A. A. 1979 Flow patterns of large eddies in a wake and in a boundary layer. *J. Fluid Mech.* **95**, 515–537.

UBEROI, M. S. & SINGH, P. I. 1975 Turbulent mixing in a two-dimensional jet. *Phys. Fluids* **18**, 764–769.

WEIR, A. D. & BRADSHAW, P. 1975 Resonance and other oscillations in the initial region of a plane turbulent jet. *I.C. Aero Rep.* 75-07, *Dept of Aeronautics, Imperial College, London.*

WYGNANSKI, I. & GUTMARK, E. 1971 Lateral motion of the two-dimensional jet boundaries. *Phys. Fluids* **14**, 1309–1311.

WYGNANSKI, I., OSTER, D., FIEDLER, H. & DZIOMBA, B. 1979 On the perseverance of a quasi-two-dimensional eddy-structure in a turbulent mixing layer. *J. Fluid Mech.* **93**, 325–335.